Capillary filling with giant liquid/solid slip: dynamics of water uptake by carbon nanotubes

Laurent Joly

Capillary filling with giant liquid/solid slip: dynamics of water uptake by carbon nanotubes

Laurent Joly[1, a)]
LPMCN, Université de Lyon; UMR 5586 Université Lyon 1 et CNRS, F-69622 Villeurbanne, France

(Dated: 18 July 2011)

This article discusses the way the standard description of capillary filling dynamics has to be modified to account for liquid/solid slip in nanometric pores. It focuses in particular on the case of a large slip length compared to the pore size. It is shown that the relevant parameter controlling the flow is neither the viscosity nor the slip length, but the friction coefficient of the liquid at the wall. Moreover in the Washburn regime, the filling velocity does not depend on the tube radius. Finally, molecular dynamics simulations suggest that this standard description fails to describe the early stage of capillary filling of carbon nanotubes by water, since viscous dissipation at the tube entrance must be taken into account.

I. INTRODUCTION

Dynamics of capillary rise is a standard case of coupling between capillarity and hydrodynamics[1,2]. The filling behavior has been investigated since the beginning of the 20th century[3–7]. In particular, the famous (Lucas-)Washburn law (neglecting the liquid inertia) states that the filling velocity decreases as the inverse square root of time. But this old problem needs to be revisited as regards nanometric pores[8,9]. Even if continuum hydrodynamics remains valid for simple liquids (including water) down to channel sizes of a typical 1 nm[10], surfaces will play an increasing role. In particular, deviations from the classical hypothesis of a no-slip boundary condition (BC) at the liquid/solid interface have been predicted theoretically and observed experimentally[11]. The simplest way to account for liquid/solid slip is the so-called 'partial slip' BC, which links the slip velocity $v_{\rm slip}$ with the shear rate at the solid surface $\partial_n v$: $v_{\rm slip} = b\,\partial_n v$, in which the slip length b is the depth inside the solid where the linear extrapolation of the velocity profile vanishes (Fig. 1.a). The partial slip BC physically stems from the continuity of tangential stress at the liquid/solid interface: the viscous shear stress exerted by the liquid on the wall $\eta\,\partial_n v$ (η being the shear viscosity) is equal to the friction force suffered by the liquid from the wall, which can be written as $F/\mathcal{A} = -\lambda\, v_{\rm slip}$ where λ is the liquid/solid friction coefficient and $\mathcal{A}$ the contact area. The slip length is accordingly related to the friction coefficient λ by the relation $b = \eta/\lambda$. For simple liquids on smooth surfaces, slip lengths up to a few tenth of nanometers have been experimentally measured[11]. Liquid-solid slip is therefore expected to significantly affect flows in channels of nanometric size, even when continuum hydrodynamics remains valid.

In recent years, many works have investigated capillary filling at the nanoscale, emphasizing the roles of dynamic contact angle, liquid inertia, and liquid-solid slip[12–26]. In this context, recent experiments[27–30] and numerical simulations[31,32] have reported slip lengths of water (and other liquids) in carbon nanotubes (CNT) much larger than the tube radius. This article seeks to investigate the way this quite special condition modifies the dynamics of capillary filling. Firstly, the full equations describing capillary filling with a partial slip boundary condition will be derived and solved. In the light of these results, orders of magnitude will then be discussed in the case of CNTs where giant liquid/solid slip has been reported. Finally this standard analytical model will be tested against molecular dynamics simulations.

II. ANALYTICAL MODEL

Equation of motion– Let's consider a cylindrical pore of radius R, in contact with a reservoir of liquid (density ρ, viscosity η), as illustrated in Fig. 1. The liquid surface tension is denoted γ, and its contact angle on the pore wall θ (it is assumed that the liquid is wetting the pore, *i.e.* $\theta < \pi/2$). The distance of the meniscus from the pore entrance is denoted L. Therefore the velocity of the meniscus V, equal to the average liquid velocity inside the pore, is related to L through: $V = \frac{{\rm d}L}{{\rm d}t}$. The filling dynamics results from the competition between a capillary force at the contact line $F_{\rm c}$, driving the motion of the liquid inside the pore, and a viscous friction force at the wall $F_{\rm v}$, slowing the liquid motion (gravity can usually be neglected at small scales). One can write the equation of motion for the liquid inside the pore:

$$\frac{{\rm d}(MV)}{{\rm d}t} = F_{\rm c} + F_{\rm v}, \tag{1}$$

where $M = \rho\pi R^2 L$ is the mass of liquid inside the pore. We will denote $\Delta\gamma = \gamma_{\rm SG} - \gamma_{\rm SL} = \gamma\cos\theta$ the capillary force per unit length at the contact line, where $\gamma_{\rm SG}$ and $\gamma_{\rm SL}$ are the solid-gas and solid-liquid surface tensions. The total capillary force is then simply given by:

$$F_{\rm c} = 2\pi R\Delta\gamma. \tag{2}$$

a) Electronic mail: laurent.joly@univ-lyon1.fr

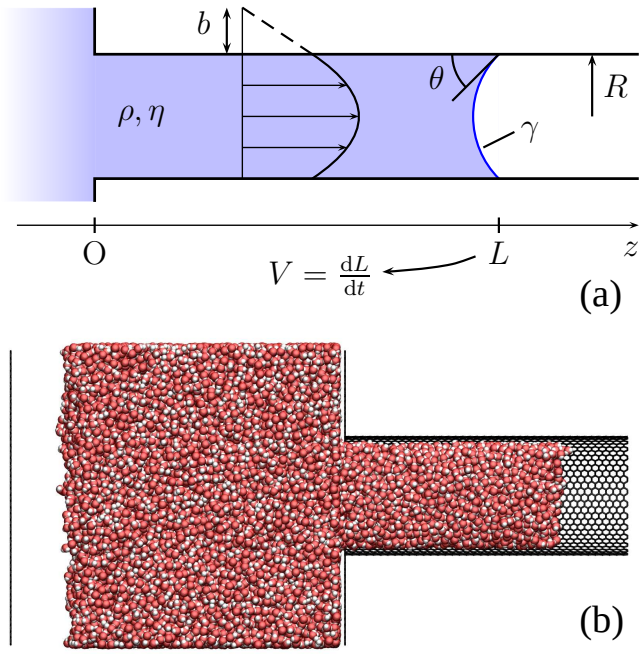

FIG. 1. (a) Schematics of the system considered. (b) Snapshot of a typical system used for the Molecular Dynamics simulations, created using VMD[33].

The friction force is given by the Poiseuille law, modified to take into account liquid/solid slip. If the flow inside the pore remains laminar, the velocity profile must assume a parabolic shape: $v_z(r) = V_{\max}(1 - Ar^2)$, where $V_{\max}$ and A are two arbitrary constants. Imposing a partial slip BC with a slip length b at the wall:

$$v_z(r = R) = -b \left.\frac{\partial v_z}{\partial r}\right|_{r=R}, \tag{3}$$

one gets:

$$v_z(r) = V_{\max}\left(1 - \frac{r^2}{R^2 + 2bR}\right). \tag{4}$$

The average velocity of the liquid inside the pore V can then be related to the maximum velocity $V_{\max}$:

$$V = \frac{1}{\pi R^2}\int_0^R v_z(r)\ 2\pi r \mathrm{d}r = \frac{V_{\max}}{2}\frac{R^2 + 4bR}{R^2 + 2bR}. \tag{5}$$

The friction force integrated over the entire liquid/solid interface is given by:

$$F_{\mathrm{v}} = \int_0^L \mathrm{d}z \int_0^{2\pi} R\mathrm{d}\theta\ \eta \left.\frac{\partial v_z}{\partial r}\right|_{r=R}. \tag{6}$$

Knowing the velocity profile (4), and expressing $V_{\max}$ as a function of V thanks to Eq. (5), this can be integrated to:

$$F_{\mathrm{v}} = -4\pi\eta L V_{\max}\frac{R^2}{R^2 + 2bR} = -\frac{8\pi\eta L V}{1 + 4b/R}. \tag{7}$$

The equation of motion (1) can finally be re-written:

$$\boxed{\frac{\mathrm{d}(\rho\pi R^2 L V)}{\mathrm{d}t} = 2\pi R\Delta\gamma - \frac{8\pi\eta L V}{1 + 4b/R}}. \tag{8}$$

Viscous regime– In micro/nanometric pores, inertia can usually be neglected compared to the viscous friction term: $\mathrm{d}(MV)/\mathrm{d}t = 0$. Eq. (8) reduces to:

$$2\pi R\Delta\gamma - \frac{8\pi\eta L V}{1 + 4b/R} = 0. \tag{9}$$

This equation can be integrated into the well-known Washburn law:

$$L^2(t) = \frac{\Delta\gamma R}{2\eta}\left(1 + \frac{4b}{R}\right)t. \tag{10}$$

Interestingly the amplification factor $1 + 4b/R$ already appeared in Washburn's original paper[4], and in several recent works[18,21,25]. However, this result is in contrast with the law used in[15], where it was assumed that the effect of liquid/solid slip could be approximated by simply increasing the effective pore radius in the expression of the drag force. Finally, one can note that the correction factor is the same one giving the amplification of flow rate in a cylindrical duct for a given pressure drop. This can be easily understood as in the viscous regime, capillary filling can also be treated as a capillary-pressure-induced Poiseuille flow.

Inertial regime– According to the Washburn law, the filling velocity V should diverge when $t \to 0$, which is physically impossible. For very short times, inertia will impose a limit to V[1,6]. In this "inertial" regime, the filled length L is very small and the viscous term can be neglected: $F_{\mathrm{v}} = 0$. It is important to consider this other limiting behavior since it may be relevant to the filling of, *e.g.* carbon nanotubes (CNT): Recent experimental[27–30] and numerical[31,32] works have indeed shown that the friction of liquids inside CNT could be extremely small. Eq. 1 becomes: $\mathrm{d}(MV)/\mathrm{d}t = F_{\mathrm{c}}$, or:

$$\frac{\mathrm{d}(\rho\pi R^2 L V)}{\mathrm{d}t} = 2\pi R\Delta\gamma \tag{11}$$

which can be solved to:

$$L(t) = \left(\frac{2\Delta\gamma}{\rho R}\right)^{1/2} t. \tag{12}$$

Of course neither the viscosity η nor the slip length b appear here since the friction term has been neglected. One could note that even the inertial regime does not appear instantaneously, essentially because the meniscus shape changes when the liquid enters into the pore. But it can be shown that the meniscus adopts a stationary shape for $L \sim R/2$[7]. Therefore, the pre-inertial regime disappears extremely fast in nanometric pores.

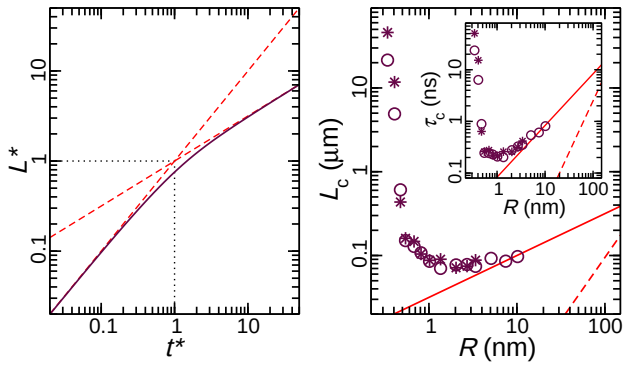

FIG. 2. (a) Full line: Evolution of the unitless filling length $L^\star = L/L_\mathrm{c}$ with unitless time $t^\star = t/\tau_\mathrm{c}$ (full solution); Dashed lines: Short-time/inertial and long-time/viscous limits. (b) Transition length L_c between inertial and viscous regimes, for water in a CNT, as a function of the tube radius R. Full line: analytical expression in the plug-flow approximation, for $\lambda = 1.2\times10^4$ Ns/m^3 (from[32]); Dashed line: no-slip limit. For very small tubes, the friction coefficient λ decreases: Data from[32] have been used. Inset: Transition time τ_c, with the same notations.

Full solution– In fact, Eq. (8) can be solved without approximation[14]. Using $LV = L\frac{\mathrm{d}L}{\mathrm{d}t} = \frac{1}{2}\frac{\mathrm{d}L^2}{\mathrm{d}t}$, it can be simplified to:

$$\frac{\mathrm{d}^2L^2}{\mathrm{d}t^2} + \frac{8\eta}{\rho R^2(1+4b/R)}\frac{\mathrm{d}L^2}{\mathrm{d}t} = \frac{4\Delta\gamma}{\rho R}. \qquad (13)$$

This non-linear equation admits the following solution[14]:

$$\frac{L(t)}{L_\mathrm{c}} = \left(\frac{t}{\tau_\mathrm{c}} + \frac{e^{-2t/\tau_\mathrm{c}}-1}{2}\right)^{1/2}, \qquad (14)$$

with:

$$\tau_\mathrm{c} = \frac{\rho R^2}{4\eta}\left(1+\frac{4b}{R}\right), \qquad (15)$$

and:

$$L_\mathrm{c} = \frac{\left(2\gamma\rho R^3\right)^{1/2}}{4\eta}\left(1+\frac{4b}{R}\right). \qquad (16)$$

One can easily check that the short time and long time limits correspond to the inertial and viscous laws, respectively (Fig. 2.a). Interestingly, this full solution provides us with the transition time τ_c and length L_c between the two regimes, where the influence of liquid/solid slippage is quantitatively taken into account.

Water inside CNT– Recent experiments[27–30] and numerical simulations[31,32] have reported surprisingly large slip lengths of water (and other liquids) in carbon nanotubes. The first experiments[27] indicated slip lengths up to tens of micrometers, even if more recent experimental[28] and numerical[32] works point to a smaller effect, with b on the order of a few hundredth of nanometers. When the slip length is much larger than the pore size: $b \gg R$, the flow inside the pore will be almost plug-like. In this regime, the shear viscosity is not expected to play a role. In fact, the viscous term F_v will only depend on the friction coefficient λ. This can be seen if one take the limit $b/R \gg 1$ in Eq. (7):

$$F_\mathrm{v} = -\frac{8\pi\eta LV}{4b/R} = -2\pi R\left(\frac{\eta}{b}\right)LV = -2\pi R\lambda LV. \qquad (17)$$

But this expression can be found directly under the assumption of a perfect plug flow, where the velocity of the liquid is everywhere equal to its average value V. The friction force over the liquid/solid contact area $\mathcal{A} = 2\pi RL$ is then simply:

$$F_\mathrm{v} = -\mathcal{A}\lambda V = -2\pi R\lambda LV. \qquad (18)$$

Generally the ratio $\eta/(1+4b/R)$ can be replaced by $\lambda R/4$ in the equation of motion (1), its solutions Eqs. (10) and (14), and the expression of the transition time (15) and transition length (16). In particular the Washburn law (in the viscous regime) becomes:

$$\boxed{L^2(t) = \frac{2\Delta\gamma}{\lambda}t}. \qquad (19)$$

In the plug-flow case, viscosity and slip length do not play a role, and the flow is only controlled by the friction coefficient. Furthermore, the filling velocity does not depend on the tube radius anymore. This important difference could be used as a clear experimental signature of a plug flow in the viscous regime.

To compute orders of magnitude, one also needs to quantify the driving force F_c. This is far from trivial: Whereas measurements of water contact angle on HOPG converge to a value of 86 °[34,35], corresponding to $\theta = 96\,°$ for water on a single graphene sheet (hence a non-wetting situation, where water should not invade CNT), there are experimental evidences that water fills at least the very small CNTs[26,36–38]. At these scales however, it is hard to apply macroscopic concepts of capillarity like surface tension and contact angle[39]. But if water indeed fills CNT, F_c will be positive and one can estimate that it will be at most on the order of $2\pi R\gamma$.

Following these considerations, one can estimate the order of magnitude for the transition time between inertial and viscous regime: $\tau_\mathrm{c} = \rho R/\lambda$. Interestingly, τ_c scales now as R in the plug-flow regime, whereas it scaled as R^2 in the no-slip regime. The (maximum) corresponding filling length is given by: $L_\mathrm{c} \sim (2\rho R\gamma)^{1/2}/\lambda$. For water ($\rho = 1\,\mathrm{g/cm^3}$, $\gamma = 0.072\,\mathrm{N/m}$), Fig. 2.b presents the evolution of L_c and τ_c with the tube radius, computed using the values of friction coefficient reported in[32]. The computed transition time and length scales are too large to be reached with molecular dynamics simulations (especially with water, involving the computation of long-range Coulomb interactions), and yet quite small from

the experimental point of view. One can conclude that molecular simulations should mainly have access to the inertial regime, whereas experiments will only be able to investigate the viscous regime. Therefore it will be very hard to confront both approaches on this kind of system. To end on an optimistic note, the extremely small friction coefficients measured numerically in (5,5) and (6,6) CNT[32] could extend the inertial domain up to time and length scales accessible by experiments (Fig. 2.b), even if these very small CNT would be quite delicate to manipulate.

III. MOLECULAR DYNAMICS SIMULATIONS AND DISCUSSION

We considered a water reservoir in contact with an initially empty CNT (Fig. 1.b). The CNT length was 10 nm, with radii ranging between 0.514 and 1.87 nm. The reservoir was bordered with two graphene sheets, at a distance large enough to ensure that the liquid water was always in equilibrium with its vapor. Periodic boundary conditions in the two directions perpendicular to the tube axis ensured that the water surface remained planar. Consequently, the pressure in the water reservoir always remained constant, at a value extremely close to zero.

The popular Amber96 force field[40] was used, with TIP3P water and water-carbon interaction modeled by a Lennard-Jones potential between oxygen and carbon atoms, with parameters $\varepsilon_{OC} = 0.114\,\text{kcal/mol}$ and $\sigma_{OC} = 3.28\,\text{Å}$. The tabulated density, surface tension and viscosity of TIP3P water at 300 K and liquid/vapor coexistence are respectively: $\rho = 0.980\,\text{g/cm}^3$, $\gamma = 0.0523\,\text{N/m}$ (from[41]), and $\eta = 0.321\,\text{mPa s}$ (from[42]). The contact angle of water on a single graphene sheet was measured independently to be $\theta = 57°$ for this model. The simulations were carried out using LAMMPS[43]. Long-range Coulomb forces were computed using the PPPM method; A timestep of 2 fs was used, unless specified. The positions of the carbon atoms were fixed (simulations with flexible and fixed walls were shown to give similar results for the statics and friction of confined liquids[34,35,44]). Water molecules were kept at a constant temperature of 300 K using a Nosé-Hoover thermostat, applied only to the degrees of freedom perpendicular to the tube axis, with a damping time of 200 fs. Alternatively a Dissipative Particle Dynamics thermostat was used (see details in the following).

Water molecules are initially disposed on a simple cubic lattice with equilibrium density, so firstly the system is equilibrated during typically 120 ps, with a plug at the tube entrance to prevent water from entering. Then the plug is removed and the evolution of the water mass inside the tube is recorded as a function of time. To compute the filling length, the mass is divided by the linear density of water inside the tube, measured once the tube is completely filled. Results for different tube radii are

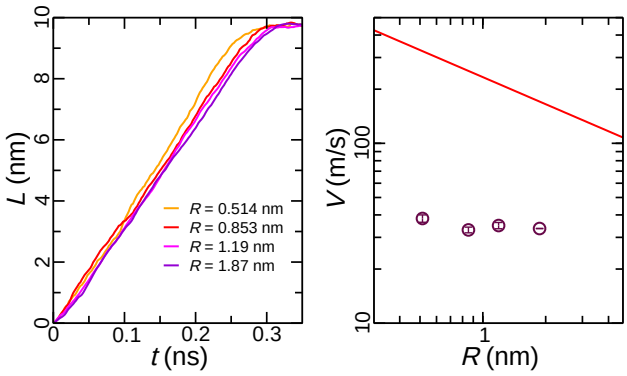

FIG. 3. (a) Evolution of the filling length L with time t, for different tube radii. (b). Filling velocity V as a function of tube radius R: Simulation data (circles) and prediction of the standard model (line), using Eq. (12).

presented in Fig. 3.a. It appears that L scales linearly with time, as expected from the model. In Fig. 3.b, the filling velocities (slope of the $L(t)$ curves) for different radii are compared to the theoretical prediction of Eq. (12). The theoretical prediction fails to describe the numerical data both quantitatively (simulated velocities are much smaller than expected) and qualitatively: While the model predicts that V should decrease as $R^{-1/2}$, the simulation shows that V does not depend significantly on the tube radius.

Obviously there is a drag force missing in the model. Even if viscosity is not expected to play a role inside the tube due to the very large slip length, its influence was nevertheless tested, using a Dissipative Particle Dynamics thermostat[45]. This amounts to adding pairwise interactions between atoms, with a dissipative force depending on the relative velocity between each pair and a random force with a Gaussian statistics. This method has the advantage of preserving hydrodynamics. Furthermore, the amplitude of the dissipative term can be tuned to modify the liquid viscosity without changing its static properties. The viscosity dependency on the dissipative term was carefully calibrated in independent simulations of shear flow of water between two silica surfaces (Fig. 4.a). For the largest dissipative terms, the timestep had to be reduced down to 0.5 fs.

The filling velocity was then measured for a given CNT, with radius 1.87 nm, varying the viscosity of the DPD-thermostated-water. On Fig. 4.b, one can observe a clear influence of viscosity on the filling velocity. Due to the very large slip length of water inside CNT, friction at the wall should be completely negligible for the filling lengths simulated. Moreover, in such a plug-flow regime, the liquid moves as a block everywhere inside the tube. Therefore, there should be no dissipation near the contact line, and consequently no dynamical change of the contact angle. Yet, even in the absence of friction inside the tube, viscous dissipation can occur at the tube entrance due to the contraction of the current lines[44,46–50].

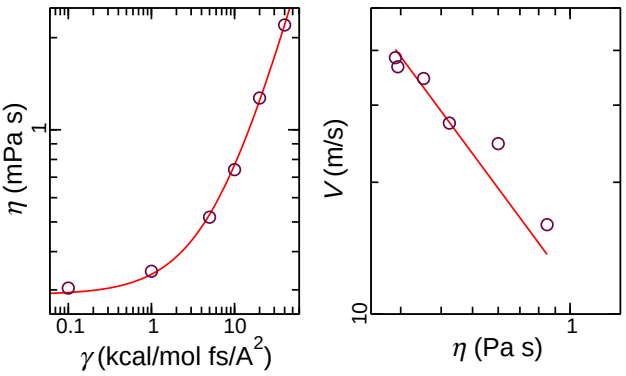

FIG. 4. (a) Calibration of viscosity η versus DPD coefficient γ: MD results (circles) and fitting curve (line), see text for detail. (b) Filling velocity V as a function of liquid viscosity η: MD results (circles) and fit with an inverse function (line).

The power dissipated by viscosity can be estimated as: $P_\mathrm{v} = \frac{\eta}{2}\int_\mathcal{V} \mathrm{d}\mathcal{V}(\partial_i v_j + \partial_j v_i)^2$. The only length scale related to the entrance of the liquid inside the tube is the tube radius, hence: $P_\mathrm{v} \propto \eta R^3 (V/R)^2 \propto \eta R V^2$. Neglecting the kinetic energy of the liquid (inertial term): $P_\mathrm{k} \propto \rho R^2 V^3$, the viscous dissipation must be equal to the power of the driving capillary force: $P_\mathrm{c} = 2\pi R \Delta\gamma V$. Finally $P_\mathrm{c} = P_\mathrm{v} \Rightarrow V \propto \Delta\gamma/\eta$. Therefore, if the filling is controlled by viscous dissipation at the entrance, the velocity should not depend on the tube radius (as observed in Fig. 3.b), and scale with the inverse of viscosity. One can check in Fig. 4 that the numerical results for V versus η are correctly fitted with an inverse function. To conclude, it seems a reasonable assumption that the early stage of capillary filling of a CNT with water is controlled by viscous dissipation at the entrance.

IV. CONCLUSION

In this article, corrections to the standard description of capillary filling of a cylindrical tube have been discussed, in a bid to account for liquid/solid slip. The dependency on the slip length of the transition time and of the transition length between the short-time/inertial regime and the viscous regime has been computed. It has then been shown that in case the slip length is much larger than the tube radius (plug-flow limit), viscosity and slip length do not play a role, and the relevant physical parameter controlling the flow is the liquid/solid friction coefficient. Moreover, scaling of the various quantities as a function of the tube radius are modified. Orders of magnitude in the particular case of CNT filling with water have been discussed. It was shown that experiments can only manage to investigate the viscous regime, whereas MD simulations can only access the short-time regime. Finally, it was shown, using MD simulations, that in the short-time limit the filling velocity is not limited by the liquid inertia, but rather by viscous dissipation at the tube entrance. Generally, friction of water inside CNT is so small that for any real flow experiments, one can expect that the hydrodynamic resistance at the tube input and output will play a significant role[50]. It could even contribute much more strongly to the total pressure drop than the friction inside the tube. In any case, measurement of flow rate versus pressure drop for CNTs of a given length can only give a higher limit for the friction coefficient inside the tube, so that measurements with different tube lengths could prove necessary.

ACKNOWLEDGMENTS

LJ thanks A.-L. Biance, L. Bocquet, K. Falk, S. Merabia, and O. Pierre-Louis for sharing data and/or for useful exchanges. This work was funded by the MIKADO grant of the Agence Nationale de la Recherche.

[1] P. G. de Gennes, F. Brochard-Wyart, and D. Quere, *Capillarity and Wetting Phenomena: Drops, Bubbles, Pearls, Waves* (Springer, 2003).
[2] B. V. Zhmud, F. Tiberg, and K. Hallstensson, "Dynamics of capillary rise," J. Colloid Interface Sci., **228**, 263–269 (2000).
[3] R. Lucas, "The time law of the capillary rise of liquids." Kolloid Z., **23**, 15–22 (1918).
[4] E. W. Washburn, "The dynamics of capillary flow." Physical Review, **17**, 273–283 (1921).
[5] C. H. Bosanquet, "On the flow of liquids into capillary tubes." Philos. Mag., **45**, 525–531 (1923).
[6] D. Quere, "Inertial capillarity," Europhys. Lett., **39**, 533–538 (1997).
[7] M. Stange, M. E. Dreyer, and H. J. Rath, "Capillary driven flow in circular cylindrical tubes," Phys. Fluids, **15**, 2587–2601 (2003).
[8] R. B. Schoch, J. Y. Han, and P. Renaud, "Transport phenomena in nanofluidics," Reviews of Modern Physics, **80**, 839–883 (2008).
[9] W. Sparreboom, A. van den Berg, and J. C. T. Eijkel, "Principles and applications of nanofluidic transport," Nature Nanotechnology, **4**, 713–720 (2009).
[10] L. Bocquet and E. Charlaix, "Nanofluidics, from bulk to interfaces," Chemical Society Reviews, **39**, 1073–1095 (2010).
[11] L. Bocquet and J. L. Barrat, "Flow boundary conditions from nano- to micro-scales," Soft Matter, **3**, 685–693 (2007).
[12] A. Marmur, "Penetration of a small drop into a capillary," J. Colloid Interface Sci., **122**, 209–219 (1988).
[13] G. Martic, F. Gentner, D. Seveno, J. De Coninck, and T. D. Blake, "The possibility of different time scales in the dynamics of pore imbibition," J. Colloid Interface Sci., **270**, 171–179 (2004).
[14] S. Supple and N. Quirke, "Molecular dynamics of transient oil flows in nanopores i: Imbibition speeds for single wall carbon nanotubes," J. Chem. Phys., **121**, 8571–8579 (2004).
[15] D. I. Dimitrov, A. Milchev, and K. Binder, "Capillary rise in nanopores: Molecular dynamics evidence for the lucas-washburn equation," Phys. Rev. Lett., **99**, 054501 (2007).
[16] P. Huber, S. Gruner, C. Schafer, K. Knorr, and A. V. Kityk, "Rheology of liquids in nanopores: A study on the capillary rise of water, n-hexadecane and n-tetracosane in mesoporous silica," European Physical Journal-special Topics, **141**, 101–105 (2007).
[17] C. Cupelli, B. Henrich, T. Glatzel, R. Zengerle, M. Moseler, and M. Santer, "Dynamic capillary wetting studied with dissipative particle dynamics," New Journal of Physics, **10**, 043009 (2008).
[18] D. Schebarchov and S. C. Hendy, "Dynamics of capillary absorption of droplets by carbon nanotubes," Physical Review E, **78**, 046309 (2008).

[19] S. Gruener, T. Hofmann, D. Wallacher, A. V. Kityk, and P. Huber, "Capillary rise of water in hydrophilic nanopores," Physical Review E, **79**, 067301 (2009).
[20] S. Ahadian, H. Mizuseki, and Y. Kawazoe, "On the kinetics of the capillary imbibition of a simple fluid through a designed nanochannel using the molecular dynamics simulation approach," J. Colloid Interface Sci., **352**, 566–572 (2010).
[21] C. Chen, C. N. Gao, L. Zhuang, X. F. Li, P. C. Wu, J. F. Dong, and J. T. Lu, "A many-body dissipative particle dynamics study of spontaneous capillary imbibition and drainage," Langmuir, **26**, 9533–9538 (2010).
[22] M. R. Stukan, P. Ligneul, J. P. Crawshaw, and E. S. Boek, "Spontaneous imbibition in nanopores of different roughness and wettability," Langmuir, **26**, 13342–13352 (2010).
[23] K. F. Wu, B. Zhou, P. Xiu, W. P. Qi, R. Z. Wan, and H. P. Fang, "Kinetics of water filling the hydrophobic channels of narrow carbon nanotubes studied by molecular dynamics simulations," J. Chem. Phys., **133**, 204702 (2010).
[24] V. N. Phan, N. T. Nguyen, C. Yang, P. Joseph, L. Djeghlaf, D. Bourrier, and A. M. Gue, "Capillary filling in closed end nanochannels," Langmuir, **26**, 13251–13255 (2010).
[25] D. Schebarchov and S. C. Hendy, "Uptake and withdrawal of droplets from carbon nanotubes," Nanoscale, **3**, 134–141 (2011).
[26] X. C. Qin, Q. Z. Yuan, Y. P. Zhao, S. B. Xie, and Z. F. Liu, "Measurement of the rate of water translocation through carbon nanotubes," Nano Letters, **11**, 2173–2177 (2011).
[27] M. Majumder, N. Chopra, R. Andrews, and B. J. Hinds, "Nanoscale hydrodynamics - enhanced flow in carbon nanotubes," Nature, **438**, 44–44 (2005).
[28] J. K. Holt, H. G. Park, Y. M. Wang, M. Stadermann, A. B. Artyukhin, C. P. Grigoropoulos, A. Noy, and O. Bakajin, "Fast mass transport through sub-2-nanometer carbon nanotubes," Science, **312**, 1034–1037 (2006).
[29] M. Whitby, L. Cagnon, M. Thanou, and N. Quirke, "Enhanced fluid flow through nanoscale carbon pipes," Nano Lett., **8**, 2632–2637 (2008).
[30] F. Du, L. T. Qu, Z. H. Xia, L. F. Feng, and L. M. Dai, "Membranes of vertically aligned superlong carbon nanotubes," Langmuir, **27**, 8437–8443 (2011).
[31] J. A. Thomas and A. J. H. McGaughey, "Reassessing fast water transport through carbon nanotubes," Nano Lett., **8**, 2788–2793 (2008).
[32] K. Falk, F. Sedlmeier, L. Joly, R. R. Netz, and L. Bocquet, "Molecular origin of fast water transport in carbon nanotube membranes: Superlubricity versus curvature dependent friction," Nano Lett., **10**, 4067–4073 (2010).
[33] W. Humphrey, A. Dalke, and K. Schulten, "VMD – Visual Molecular Dynamics," J. Molec. Graphics, **14**, 33–38 (1996), http://www.ks.uiuc.edu/Research/vmd/.
[34] A. Alexiadis and S. Kassinos, "Molecular simulation of water in carbon nanotubes," Chemical Reviews, **108**, 5014–5034 (2008).
[35] T. Werder, J. H. Walther, R. L. Jaffe, T. Halicioglu, and P. Koumoutsakos, "On the water-carbon interaction for use in molecular dynamics simulations of graphite and carbon nanotubes," J. Phys. Chem. B, **107**, 1345–1352 (2003).
[36] A. I. Kolesnikov, J. M. Zanotti, C. K. Loong, P. Thiyagarajan, A. P. Moravsky, R. O. Loutfy, and C. J. Burnham, "Anomalously soft dynamics of water in a nanotube: A revelation of nanoscale confinement," Phys. Rev. Lett., **93**, 035503 (2004).
[37] H. Kyakuno, K. Matsuda, H. Yahiro, Y. Inami, T. Fukuoka, Y. Miyata, K. Yanagi, Y. Maniwa, H. Kataura, T. Saito, M. Yumura, and S. Iijima, "Confined water inside single-walled carbon nanotubes: Global phase diagram and effect of finite length," J. Chem. Phys., **134**, 244501 (2011).
[38] T. A. Pascal, W. A. Goddard, and Y. Jung, "Entropy and the driving force for the filling of carbon nanotubes with water," PNAS (2011), doi:10.1073/pnas.1108073108.
[39] J. W. van Honschoten, N. Brunets, and N. R. Tas, "Capillarity at the nanoscale," Chem. Soc. Rev., **39**, 1096–1114 (2010).
[40] W. D. Cornell, P. Cieplak, C. I. Bayly, I. R. Gould, K. M. Merz, D. M. Ferguson, D. C. Spellmeyer, T. Fox, J. W. Caldwell, and P. A. Kollman, "A 2nd generation force-field for the simulation of proteins, nucleic-acids, and organic-molecules," J. Am. Chem. Soc., **117**, 5179–5197 (1995).
[41] C. Vega and E. de Miguel, "Surface tension of the most popular models of water by using the test-area simulation method," J. Chem. Phys., **126**, 154707 (2007).
[42] M. A. Gonzalez and J. L. F. Abascal, "The shear viscosity of rigid water models," J. Chem. Phys., **132**, 096101 (2010).
[43] S. Plimpton, "Fast parallel algorithms for short-range molecular-dynamics," J. Comp. Phys., **117**, 1–19 (1995), http://lammps.sandia.gov/.
[44] J. A. Thomas and A. J. H. McGaughey, "Water flow in carbon nanotubes: Transition to subcontinuum transport," Phys. Rev. Lett., **102**, 184502 (2009).
[45] R. D. Groot and P. B. Warren, "Dissipative particle dynamics: Bridging the gap between atomistic and mesoscopic simulation," J. Chem. Phys., **107**, 4423–4435 (1997).
[46] R. A. Sampson, "On stokes's current function," Phil. Trans. R. Soc. Lond. A, **182**, 449–518 (1891).
[47] F. C. Johansen, "Flow through pipe orifices at low reynolds numbers," Proc. R. Soc. Lond. A, **126**, 231–245 (1930).
[48] H. L. Weissberg, "End correction for slow viscous flow through long tubes," Physics of Fluids, **5**, 1033–1036 (1962).
[49] E. A. van Nierop, B. Scheid, and H. A. Stone, "On the thickness of soap films: an alternative to frankel's law," Journal of Fluid Mechanics, **602**, 119–127 (2008).
[50] T. B. Sisan and S. Lichter, "The end of nanochannels," (2011), arXiv:1107.3081v1 [physics.flu-dyn].